

GSI-Preprint-2000-12

# Non-local effects in kaonic atoms

Matthias Lutz<sup>a</sup> and Wojciech Florkowski<sup>b</sup>

<sup>a</sup>*Gesellschaft für Schwerionenforschung GSI, Postfach 110552, D-64220  
Darmstadt, Germany*

<sup>b</sup>*H. Niewodniczański Institute of Nuclear Physics, ul. Radzikowskiego 152,  
PL-31-342 Kraków, Poland*

---

## Abstract

Optical potentials with non-local (gradient) terms are used to describe the spectra of kaonic atoms. The strength of the non-local terms is determined from a self consistent many-body calculation of the kaon self energy in nuclear matter based on s-wave kaon nucleon interactions. The optical potentials show strong non-linearities in the nucleon density and sizeable non-local terms. We find that the non-local terms are quantitatively important and the results depend strongly on the way the gradient terms are arranged. Phenomenologically successful description is obtained for p-wave like optical potentials. It is suggested that the microscopic form of the non-local interaction terms is obtained systematically by means of a semi-classical expansion of the nucleus structure. We conclude that a microscopic description of kaonic atom data requires further detailed studies of the microscopic  $K^-$  nuclear dynamics.

---

## 1 Introduction

Kaonic atom data provide a valuable consistency check on any microscopic theory of the  $K^-$  nucleon interaction in nuclear matter. We therefore apply the microscopic approach, developed by one of the authors in [1], to kaonic atoms. The description of the nuclear level shifts in  $K^-$  atoms has a long history. For a recent review see [2]. We recall here the most striking puzzle. In the extreme low-density limit the nuclear part of the optical potential,  $U_{\text{opt.}}$ , is determined by the s-wave  $K^-N$  scattering length:

$$2\mu U_{\text{opt.}}(\vec{r}) = -4\pi \left(1 + \frac{m_K}{m_N}\right) a_{KN} \rho(r) \quad (1)$$

with  $a_{KN} = \frac{1}{4}a_{KN}^{(I=0)} + \frac{3}{4}a_{KN}^{(I=1)} \simeq (-0.18 + 0.67i)$  fm, the nucleus density profile  $\rho(r)$  and the reduced kaon mass  $\mu$  of the  $K^-$  nucleus system. As shown by Friedman, Gal and Batty [3] kaonic atom data can be described with a large attractive effective scattering length  $a_{\text{eff.}} \simeq (0.63 + 0.89i)$  fm, which is in direct contradiction to the low-density optical potential (1). The present data set on kaonic level shifts include typically the 3d→2p transition for light nuclei and the 4f→3d transition for heavy nuclei. Deeply bound kaonic bound states in an s-wave have so far been not observed. Since a  $K^-$  bound in a p-wave at a nucleus probes dominantly the low-density tail of the nucleus profile one may conclude that the optical potential must exhibit a strong non-linear density characteristic at rather low density.

A further complication was pointed out already by Thies [4], who demonstrated that for example in the kaonic  $^{12}_6C$  system non-local effects may be important. In fact a reasonable description of kaonic atom level shifts was achieved by Mizoguchi, Hirenzaki and Toki [5] with a phenomenological non-local optical potential of the form

$$2\mu U_{\text{opt.}}(\vec{r}, \vec{\nabla}) = -4\pi \left(1 + \frac{m_K}{m_N}\right) \left(a_{K-N} \rho(r) - b \vec{\nabla} \rho(r) \cdot \vec{\nabla}\right), \quad (2)$$

where the parameter  $b \simeq (0.47 + i 0.30)$  fm<sup>3</sup>.

Though it has been long anticipated that the  $\Lambda(1405)$  resonance plays a key role [5,6] a microscopic description of kaonic atom data remains a challenge. Obviously an important ingredient of any such attempt must be a proper many-body treatment of the  $\Lambda(1405)$  resonance structure in nuclear matter.

## 2 Kaon self energy in nuclear matter

In this section we prepare the ground for our study of kaonic atoms. Of central importance is the kaon self energy,  $\Pi_K(\omega, \vec{q}; \rho)$ , evaluated in nuclear matter. Here we introduce the self energy relative to all vacuum polarization effects, i.e.  $\Pi_K(\omega, \vec{q}; 0) = 0$ .

First we recall results for the kaon self energy as obtained in a self consistent many-body calculation based on microscopic s-wave kaon-nucleon interactions. For the details of this microscopic approach we refer to [1]. We identify the  $K^-$ -nucleus optical potential  $V_{\text{opt.}}(\vec{q})$  by

$$2E_K(\vec{q}) V_{\text{opt.}}(\vec{q}) = \Pi_K(\omega = E_K(\vec{q}), \vec{q}), \quad (3)$$

where  $E_K(\vec{q}) = (m_K^2 + \vec{q}^2)^{1/2}$  is the free space kaon energy. In Fig. 1 we present the result of [1] at nuclear saturation density. We point out that the

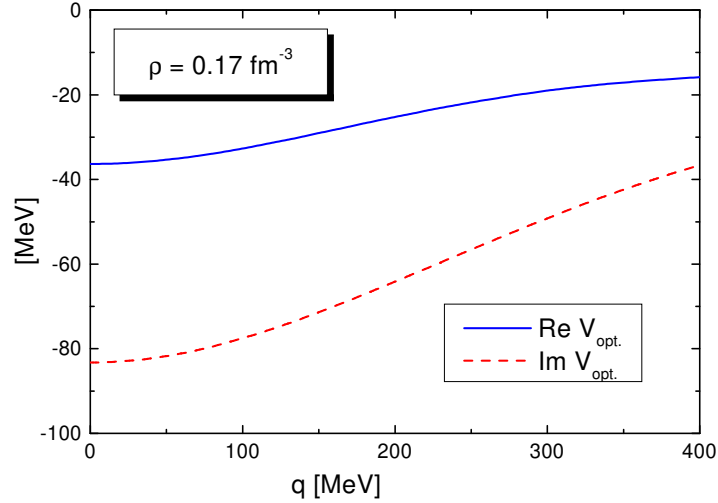


Fig. 1. The  $K^-$  nuclear optical potential,  $V_{\text{opt.}}(\vec{q})$ , plotted as a function of the kaon three momentum. The nuclear density is  $\rho = 0.17 \text{ fm}^{-3}$ .

real part of our optical potential exhibits rather moderate attraction of less than 40 MeV. On the other hand we find a rather strong absorptive part of the optical potential. This is in disagreement with recent work by Friedman, Gal, Mares and Cieply [7]. We recall that in [1] the quasi-particle energy for a  $K^-$  at rest was found to be 380 MeV at nuclear saturation density and that the large attraction in the quasi-particle energy is consistent with the moderate attraction in the optical potential. It merely reflects the strong energy dependence of the kaon self energy induced by the  $\Lambda(1405)$  resonance. Such important energy variations are typically missed in a mean field approach. Hence, a proper treatment of the pertinent many-body effects is mandatory.

We analyze the self energy as probed in kaonic atoms in more detail. Before we proceed it is important to straighten out the relevant scales. Since the typical binding energy of a  $K^-$  bound at a nucleus in a p-wave is of the order of 0.5 MeV the typical kaon momentum is estimated to be roughly 20 MeV. We then expect the relevant nuclear Fermi momentum  $k_F$  to be larger than the kaon momentum  $|\vec{q}| < k_F$ . For the study of kaonic level shifts it is therefore useful to introduce the effective scattering length  $a_{\text{eff.}}(k_F)$  and the effective slope parameters  $b_{\text{eff.}}(k_F)$  and  $c_{\text{eff.}}(k_F)$

$$\begin{aligned} \Pi_K(\omega, \vec{q}) = & -\frac{8}{3\pi} \left( 1 + \frac{m_K}{m_N} \right) \left( a_{\text{eff.}}(k_F) k_F^3 + b_{\text{eff.}}(k_F) k_F^2 \vec{q}^2 \right) \\ & + \frac{8}{3\pi} \left( 1 + \frac{m_K}{m_N} \right) c_{\text{eff.}}(k_F) k_F^2 (\omega - m_K) \\ & + \mathcal{O} \left( \vec{q}^4, (\omega - m_K)^2, \vec{q}^2 (\omega - m_K) \right), \end{aligned} \quad (4)$$

where we expanded the kaon self energy for small momenta with  $|\vec{q}| < k_F$  and energies close to  $m_K$ <sup>1</sup>. It is instructive to derive the model independent low-density limit of the slope parameters:

$$\begin{aligned} b_{\text{eff.}}(k_F = 0) &= \frac{1}{8\pi} \left( \frac{2}{1-\kappa} + \frac{7-3\kappa^2}{1-\kappa^2} \frac{\log|\kappa|}{1-\kappa} \right) \left( (a_{KN}^{(I=0)})^2 + 3(a_{KN}^{(I=1)})^2 \right), \\ c_{\text{eff.}}(k_F = 0) &= \frac{3m_K}{4\pi} \frac{\log|\kappa|}{1-\kappa} \left( (a_{KN}^{(I=0)})^2 + 3(a_{KN}^{(I=1)})^2 \right), \end{aligned} \quad (5)$$

which is given in terms of the kaon-nucleon scattering lengths and the ratio  $\kappa = m_K/m_N$ . As demonstrated in the appendix these limits are determined by the

<sup>1</sup> We emphasize that expressions (4,5) do not contradict the low-density theorem since we explicitly assume  $q < k_F$  in the definition of  $b_{\text{eff.}}(k_F)$  and  $c_{\text{eff.}}(k_F)$ . Our optical potential is then incorrect for  $k_F < q \sim 20$  MeV where we assume a typical 3-momentum of the kaon probed in K-atoms. However, the non-local terms involving a gradient acting on the density profile are peaked at the nucleus surface where  $k_F \gg q \sim 20$  MeV. We thus conclude that our expansion is meaningful in the region where the non-local effects contribute. The systematic error we encounter with our optical potential, incorrect only in the rather small density interval  $0 < k_F < 20$  MeV, is certainly insignificant since the optical potential is already tiny by itself in this region.

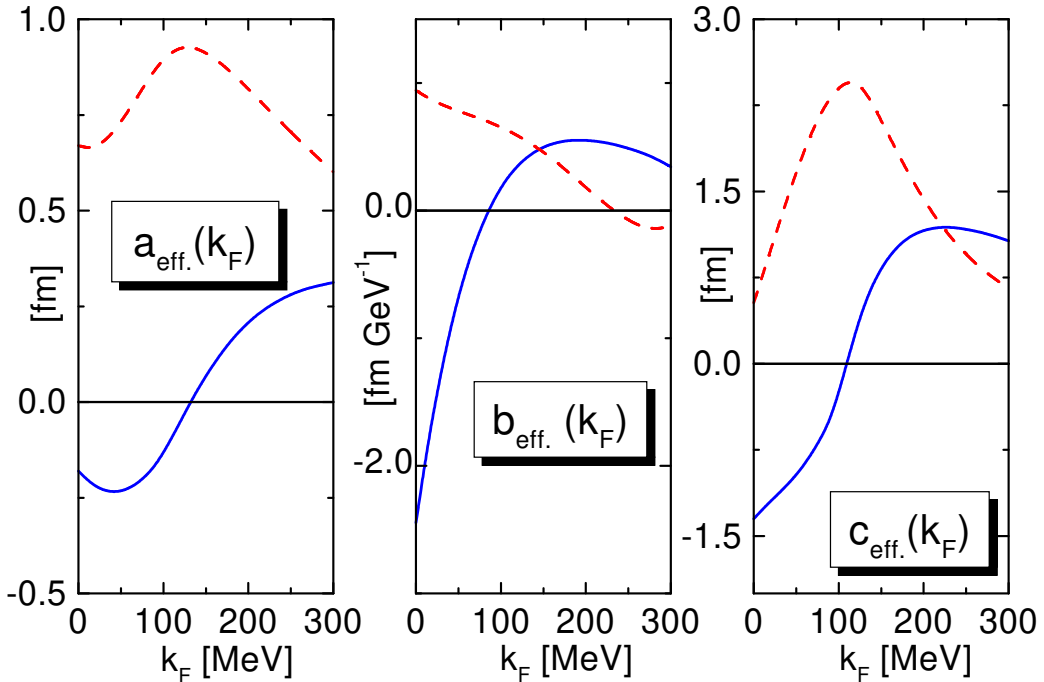


Fig. 2. The effective scattering length  $a_{\text{eff.}}(k_F)$  and effective slope parameters  $b_{\text{eff.}}(k_F)$  and  $c_{\text{eff.}}(k_F)$  as defined in (4). The solid and dashed lines represent the real and imaginary parts, respectively.

Pauli blocking effect which characterizes the leading medium modification of the kaon-nucleon scattering process. Using the values for the scattering lengths we obtain  $b_{\text{eff.}}(0) \simeq (-2.45 + i 0.95) \text{ fm GeV}^{-1}$  and  $c_{\text{eff.}}(0) \simeq (-1.35 + i 0.53) \text{ fm}$ .

In Fig. 2 the effective scattering length and the slope parameters are presented as extracted numerically from the self consistent calculation of [1]. The real part of the effective scattering length  $a_{\text{eff.}}(k_F)$  changes sign as the density is increased. At large densities we find an attractive effective scattering length in qualitative agreement with previous work [8]. Note that the quantitative differences of the works [8] and [1] are most clearly seen in the imaginary part of the effective scattering length in particular at small density. A even more recent calculation by Ramos and Oset [15] confirms the results of [1] at the qualitative level. The quantitative differences will be discussed in the next section. Most dramatic are the non-linear density effects in the effective slope parameters  $b_{\text{eff.}}(k_F)$  and  $c_{\text{eff.}}(k_F)$ , not considered in [8,9,15].

The non-trivial changes in the effective scattering length and effective slope parameters are the key elements of our microscopic approach to the kaonic atom level shifts.

### 3 Non-local optical potential: phenomenology

In this section, in order to make an estimate of non-local effects in kaonic atoms, we calculate the spectra with an optical potential  $U_{\text{opt.}}(r, \vec{\nabla})$  deduced from the kaon self energy (4) but use a phenomenological Ansatz for its non-local structure. Our starting point is the Klein-Gordon equation

$$\vec{\nabla}^2 \phi(r) + \left[ \left( \mu - E - \frac{i\Gamma}{2} - V_{\text{e.m.}}(r) \right)^2 - \mu^2 \right] \phi(r) = 2\mu U_{\text{opt.}}(r, \vec{\nabla}) \phi(r), \quad (6)$$

where  $E$  and  $\Gamma$  are the binding energy and width of the kaonic atom, whereas  $\mu$  is the reduced kaon mass in the  $K^-$  nucleus system. The electromagnetic potential  $V_{\text{e.m.}}$  is the sum of the Coulomb potential and the Uehling and Källen-Sabry vacuum polarization potentials [10] folded with the nucleus density profile. The nuclear densities are taken from [3], where they are obtained by unfolding a gaussian proton charge distribution from the tabulated nuclear charge distributions [11]. We solve the Klein-Gordon equation (6) using the computational procedure of Krell and Ericson [12].

For the optical potential  $U_{\text{opt.}}(r, \vec{\nabla})$ , appearing on the right-hand-side of (6), we make the following Ansatz:

Nucleus		LDT	$U_{\text{opt.}}^{(0)}$	$U_{\text{opt.}}^{(1)}$	$U_{\text{opt.}}^{(2)}$	$U_{\text{opt.}}^{(3)}$	RO+L	experiment
${}_{\frac{10}{5}}\text{B}$	$-\Delta E_{\text{nucl.}}$	174	222	238	236	-128	237	$208 \pm 35$ [13]
	$\Gamma$	322	441	405	569	11	713	$810 \pm 100$ [13]
${}_{\frac{12}{6}}\text{C}$	$-\Delta E_{\text{nucl.}}$	475	603	638	638	-218	674	$590 \pm 80$ [13]
	$\Gamma$	761	1022	926	1342	-38	1694	$1730 \pm 150$ [13]
${}_{\frac{27}{13}}\text{Al}$	$-\Delta E_{\text{nucl.}}$	92	115	130	141	-128	135	$130 \pm 50$ [14]
	$\Gamma$	220	293	282	395	-52	478	$490 \pm 160$ [14]
${}_{\frac{32}{16}}\text{S}$	$-\Delta E_{\text{nucl.}}$	497	625	683	729	-378	748	$550 \pm 60$ [13]
	$\Gamma$	1023	1324	1264	1748	-41	2105	$2330 \pm 200$ [13]

Table 1

Collection of our results for different nuclei. The energy level shifts  $\Delta E_{\text{nucl.}}$  and widths are all given in eV. LDT denotes the results obtained with the use of the low-density theorem with  $a_{KN} = (-0.18 + i 0.67)$  fm. The last column gives the empirical value of [13,14]. The results obtained with the optical potentials (7) are listed in the columns denoted by  $U_{\text{opt.}}^{(0)}$ ,  $U_{\text{opt.}}^{(1)}$ ,  $U_{\text{opt.}}^{(2)}$  and  $U_{\text{opt.}}^{(3)}$ , respectively. RO+L is the result obtained with  $a[\rho]$  given by Ramos and Oset [15], and  $b[\rho]$  given in [1].

$$\begin{aligned}
U_{\text{opt.}}^{(i)} &= U_{\text{opt.}}^{(0)} + V_i, \quad 2\mu U_{\text{opt.}}^{(0)} = -4\pi \left(1 + \frac{m_K}{m_N}\right) a[\rho(r)] \rho(r), \\
2\mu V_1 &= 4\pi \left(1 + \frac{m_K}{m_N}\right) b[\rho(r)] \rho(r) \vec{\nabla}^2, \\
2\mu V_2 &= 4\pi \left(1 + \frac{m_K}{m_N}\right) b[\rho(r)] \vec{\nabla} \rho(r) \cdot \vec{\nabla}, \\
2\mu V_3 &= 4\pi \left(1 + \frac{m_K}{m_N}\right) b[\rho(r)] [\vec{\nabla}^2 \rho(r)]. \tag{7}
\end{aligned}$$

In contrast to the approach of [5] we do not fit the spectrum. The effective scattering length  $a[\rho]$  and the effective slope parameter  $b[\rho]$  in (7) are determined by the expansion of the  $K^-$  self energy at small momenta (see (4)): we identify  $a = a_{\text{eff.}}$  and  $b = b_{\text{eff.}}/k_F$ . The optical potentials (7) follow from (4) with  $\vec{q}$  replaced by the momentum operator  $-i\vec{\nabla}$ . Of course, this heuristic procedure is not unique and may lead to different ways of ordering of the gradients. For this reason we study three different cases separately. Although our procedure of constructing the optical potential is not strict, it allows us to make an estimate of the magnitude of the non-local effects, usually neglected in other approaches. A more systematic derivation of the non-local part of the optical potential is suggested in the subsequent section.

The nuclear energy shift  $\Delta E_{\text{nucl.}}$  and the width  $\Gamma$  of the 3d→2p transition ( ${}^{10}_{\text{B}}$ ,  ${}^{12}_{\text{C}}$ ) and the 4f→3d transition ( ${}^{27}_{\text{Al}}$ ,  ${}^{32}_{\text{S}}$ ) are presented in Tab. 1. In the second column (LDT) we recall the results obtained with the optical potential determined by the low-density theorem (1). In the next column we present the results obtained with the effective scattering length  $a = a_{\text{eff.}}$ , as shown in Fig. 2. The use of the density dependent scattering length improves the agreement with the empirical data as compared to the density independent scattering length. In particular the level widths increase towards the empirical values. In the next three columns we show the results obtained with the non-local potentials of (7) with  $b = b_{\text{eff.}}/k_F$ . For all considered nuclei we observe the same type of the change in the spectrum: the effect of  $U_{\text{opt.}}^{(1)}$  is small,  $U_{\text{opt.}}^{(2)}$  leads to a further (desired) increase of the widths, whereas  $U_{\text{opt.}}^{(3)}$  makes the energy level shifts negative – in no way comparable to the data. In contrast to  $U_{\text{opt.}}^{(1)}$ , the effects of both  $U_{\text{opt.}}^{(2)}$  and  $U_{\text{opt.}}^{(3)}$  are very large. They change the binding energies and widths by hundreds of eV.

The best results are obtained for the optical potential  $U_{\text{opt.}}^{(2)}$ . The non-local part of this potential leaves the energy shift almost unchanged but the widths become substantially larger as compared to the local potential  $U_{\text{opt.}}^{(0)}$ . This is an effect leading towards the proper spectrum. However, in our case the strength of  $b$  is too small to obtain a completely successful agreement with data. An improved phenomenological description of the selected cases is achieved if the effective scattering length  $a_{\text{eff.}}$  of Ramos and Oset [15] is combined with the effective slope parameter  $b_{\text{eff.}}$  of Fig. 2. The results, shown in the second last row of Tab. 1, agree remarkably well with the data. Of course it is not consistent to combine the two different calculations [1,15]. The last column is included only to demonstrate that there may be many different ways to describe the K-atom data in a phenomenological approach.

We emphasize that we do not advocate that either of the three phenomenological gradient orderings is realistic. Tab. 1 is included in this work to demonstrate that non-local effects are important and in particular that it is crucial to derive the proper gradient ordering systematically. Furthermore we point out that the expansion of the kaon self energy in small momenta  $q$  in (4) requires that the contribution of the region  $0 < k_F < q \simeq 20$  MeV to the kaonic level shifts is insignificant. In order to verify this assumption we artificially modified the slope function such that it is zero at  $k_F = 0$  but agrees to good accuracy with  $b_{\text{eff.}}(k_F)$  for  $k_F > 50$  MeV. This is achieved with:

$$b_{\text{eff.}}(k_F) \rightarrow \sqrt{\frac{k_F^2}{(20 \text{ MeV})^2 + k_F^2}} b_{\text{eff.}}(k_F) . \quad (8)$$

We considered the implication of the modified slope function (8) for the level shift of the  ${}^{12}_{\text{C}} K^-$  system. Whereas the optical potentials  $U_{\text{opt.}}^{(1)}$  and  $U_{\text{opt.}}^{(2)}$  are

found rather insensitive to the modification of  $b_{\text{eff.}}(k_F)$  according to (8), the level shift and width change by less than 2%, the optical potential  $U_{\text{opt.}}^{(3)}$  shows a strong effect. The latter potential leads to  $\Delta E = -20$  eV and  $\Gamma = 206$  eV and thus introduces an uncertainty of about 200 eV in the level shift and width. Note that since  $U_{\text{opt.}}^{(3)}$  probes to some extent the extreme surface region of the nucleus a systematic reduction of the associated uncertainties requires the use of density profiles which are realistic also in the extreme surface region. We emphasize, however, that the uncertainty for our final optical potential, for which the proper gradient ordering will be derived in the next section, is expected to be much reduced. This follows since the potentially large term  $U_{\text{opt.}}^{(3)}$  necessarily contributes with reduced weight. For example using the symmetrized form of  $U_{\text{opt.}}^{(1)}$ ,  $U_{\text{opt.}}^{(2)}$  and  $U_{\text{opt.}}^{(3)}$ , as suggested by a density independent s-wave interaction [1], already reduces this uncertainty by a factor of four.

It is instructive to compare our results with the analysis of Ramos and Oset [15]. In their approach the real part  $a[\rho]$  becomes positive at somewhat smaller densities, as compared to the calculation [1]. A more rapid change of  $\text{Re } a[\rho]$  leads to a stronger attraction of the optical potential  $U_{\text{opt.}}^{(0)}$  and better agreement with empirical level shifts [16]<sup>2</sup>. We point out that the recent calculations [17,16] are not conclusive since first, they ignore the important non-local structure of the optical potential and second, the optical potential is still subject to sizeable uncertainties from the poorly determined underlying microscopic kaon-nucleon interaction. Strong non-local effects are an immediate consequence of the  $\Lambda(1405)$ -resonance structure and an important part of any microscopic description of kaonic atom data. The uncertainties in the optical potential reflect the poorly determined subthreshold kaon-nucleon scattering amplitudes. The isospin zero amplitude of [15] and [1] differ by almost a factor two in the vicinity of the  $\Lambda(1405)$ -resonance. Naively one might expect that the amplitudes of [1] are more reliable since they are constructed to reproduce the amplitudes of [8] which are based on a chiral  $SU(3)$  analysis of the kaon-nucleon scattering data to chiral order  $Q^2$  as compared to the analysis of Ramos and Oset, which considers only the leading order  $Q$ . On the other hand the amplitudes of [15] include further channels implied by  $SU(3)$ -symmetry but not included in the amplitudes of [8]. Also the work by Ramos and Oset includes the effect of an in-medium modified pion propagation not included in [1]. Note, however that such effects are not too large at small density. Clearly a reanalysis of the scattering data and the self consistent many-body approach in an improved chiral  $SU(3)$  scheme is highly desirable [18].

---

<sup>2</sup> Note that in [17] an unrealistic density profile is used for light nuclei. If the effective scattering length of [15] and the density profile (24) is used for the  $^{12}_6\text{C K}^-$  system the nuclear level shift is  $\Delta E_{\text{nucl.}} = -623$  eV and  $\Gamma = 1290$  eV.

## 4 Semi-classical expansion

In this section we suggest to systematically construct the non-local part of the optical potential by a semi-classical expansion of the nucleus structure. In the previous section we have demonstrated that the ordering of the gradient terms has dramatic influence on the kaonic level shifts. Naively one may conjecture that the gradient ordering should be s-wave like since the vacuum kaon-nucleon interaction is s-wave dominated. A perturbative s-wave interaction would give rise to the gradient ordering suggested in [1] in contrast to the phenomenological successful Kisslinger potential [19] employed in [5]. However, since the kaon self energy is obtained in a non-perturbative many-body approach it is not obvious as to which gradient ordering to choose. In particular it is unclear to what extent the gradients are supposed to act on the function  $b_{\text{eff.}}(k_F)$  in (4). Since  $b_{\text{eff.}}(k_F)$  is a rapidly varying function in the nuclear density such effects have to be considered.

The starting point of our semi-classical approach is the Klein-Gordon equation

$$\left[ \vec{\nabla}^2 - \mu^2 + (\omega - V_{\text{e.m.}}(r))^2 \right] \phi(\vec{r}) = 2\mu \int d^3r' U_{\text{opt.}}(\omega, \vec{r}, \vec{r}') \phi(\vec{r}') \quad (9)$$

with the non-local  $K^-$  nuclear optical potential  $U_{\text{opt.}}(\vec{r}, \vec{r}')$  and  $\omega = \mu - E - \frac{i\Gamma}{2}$ . Since the binding energy  $E$  of a kaonic atom is of the order of hundreds of keV it will be justified to expand the nuclear optical potential in the kaon energy  $\omega$  around the reduced kaon mass  $\mu$ . Here we exploit the obvious fact that the nuclear part of the potential varies extremely smoothly at that scale.

In order to derive the form of the non-locality in the nuclear optical potential it is useful to consider the in-medium kaon-nucleon scattering process. The s-wave  $K^-$ -nucleon interaction of [1] implies that the scattering amplitude,  $T_{KN}(\omega, \vec{q})$ , depends exclusively on the sum of initial kaon and nucleon momenta  $\vec{q}$ , and energies  $\omega$ . Close to the kaon-nucleon threshold the former can therefore be represented by the density dependent coefficients  $a_{KN}(\rho)$ ,  $b_{KN}(\rho)$  and  $c_{KN}(\rho)$

$$T_{KN}(\omega, \vec{q}; \rho) = 4\pi \left( 1 + \frac{m_K}{m_N} \right) \left( a_{KN}(\rho) + b_{KN}(\rho) \vec{q}^2 - c_{KN}(\rho) (\omega - m_N - m_K) + \dots \right), \quad (10)$$

where we suppress higher order terms for simplicity. We note that at vanishing baryon density one expects from covariance  $2(m_N + m_K)b_{KN} = c_{KN}$ . In the nuclear medium, however, the functions  $b_{KN}(\rho)$  and  $c_{KN}(\rho)$  are independent

quantities. In the appendix the model independent low-density characteristic is derived:

$$\begin{aligned} b_{KN}(\rho) &= -\frac{1}{6\pi} \frac{3\kappa-1}{(1+\kappa)^2} \frac{1}{k_F} \left( \left(a_{KN}^{(I=0)}\right)^2 + 3 \left(a_{KN}^{(I=1)}\right)^2 \right) + \mathcal{O}(k_F^0) , \\ c_{KN}(\rho) &= -\frac{1}{\pi} \frac{m_K}{1+\kappa} \frac{1}{k_F} \left( \left(a_{KN}^{(I=0)}\right)^2 + 3 \left(a_{KN}^{(I=1)}\right)^2 \right) + \mathcal{O}(k_F^0) . \end{aligned} \quad (11)$$

It should not come as a surprise that we find  $b_{KN} \sim 1/k_F$  and  $c_{KN} \sim 1/k_F$  at small density. The leading term follows upon expansion of the scattering amplitude in powers of small momenta followed by the low density expansion. For details we refer to the appendix. In fact the expansion in (10) stops to converge at  $k_F < q$ . Since the scattering amplitude leads to the kaon self energy via

$$\Pi_K(\omega, \vec{q}) = -4 \int_0^{k_F} \frac{d^3 p}{(2\pi)^3} T_{KN} \left( \omega + m_N + \frac{\vec{p}^2}{2m_N}, \vec{q} + \vec{p} \right) \quad (12)$$

we conclude that at small density (with  $k_F < 50$  MeV) an accurate representation of the kaon self energy requires an infinite number of terms in (10). A manifestation of this fact is that  $c_{\text{eff.}} \neq k_F c_{KN}$  and  $b_{\text{eff.}} \neq k_F b_{KN}$  at small density. Note, however, that at somewhat larger density with  $50 \text{ MeV} < k_F < 300 \text{ MeV}$ , we obtain a faithful representation of the self energy keeping only a few terms in (10)<sup>3</sup>. This observation is a key element in our derivation of the optical potential since it leads to a unique non-local part of the optical potential.

In order to proceed and derive the non-local kaon optical potential we generalize (12), which holds for infinite homogeneous nuclear matter, to the non-local system of a nucleus (see e.g. [4]):

$$2\mu U_{\text{opt.}}(\omega, \vec{r}, \vec{r}') = - \sum_n \chi_n^\dagger(\vec{r}) T \left( \omega - V_{\text{e.m.}}(\vec{r}') + E_n, \vec{r}, \vec{r}' \right) \chi_n(\vec{r}') . \quad (13)$$

Here we introduced the non-local amplitude  $T(\omega, \vec{r}, \vec{r}')$  and the nucleon wave function  $\chi_n(\vec{r})$  for a given nucleus in a shell model description.  $E_n$  is the energy of the single particle wave function and the index  $n$  sums all occupied shell model states of the nucleus.

---

<sup>3</sup> Our optical potential will finally be expressed directly in terms of  $b_{\text{eff.}}(k_F)$  and  $c_{\text{eff.}}(k_F)$  defined in (4) and extracted numerically from the kaon self energy of [1] (see discussion below (20)).

To make contact with the formalism for homogeneous nuclear matter it is useful to transform the amplitude  $T(\omega, \vec{q}; \vec{R})$  to momentum space

$$T(\omega, \vec{r}, \vec{r}') = \int \frac{d^3 q}{(2\pi)^3} e^{i \vec{q} \cdot (\vec{r} - \vec{r}')} T(\omega, \vec{q}; \vec{R}) \quad (14)$$

with  $\vec{R} = (\vec{r} + \vec{r}')/2$ . In the limit of infinite and homogeneous nuclear matter the amplitude  $T(\omega, \vec{q}; \vec{R})$  does not depend on  $\vec{R}$  and equals the previously analyzed amplitude of (10). For the non-local system we identify:

$$T_{KN}(\omega, \vec{q}; \rho(\vec{R})) = T(\omega, \vec{q}; \vec{R}) \quad (15)$$

with  $\rho(\vec{R})$  the density profile of the nucleus.

We now aim at a shell model independent representation of the non-local optical potential by rewriting it in terms of the nuclear density profile of the nucleus. Consider first the term proportional to  $b_{KN} \vec{q}^2$  in (10). We rewrite its contribution to the optical potential by means of the semi-classical expansion

$$\begin{aligned} b_{KN}(\vec{R}) \sum_n \chi_n^\dagger(\vec{r}) \chi_n(\vec{r}') \vec{\nabla}_{\vec{r}'} \cdot \vec{\nabla}_{\vec{r}'} \delta^3(\vec{r} - \vec{r}') \\ = \left( \frac{1}{4} \Delta \rho(r) b_{KN}(r) - \frac{3}{5} b_{KN}(r) k_F^2(r) \rho(r) - \frac{1}{12} b_{KN}(r) \Delta \rho(r) \right. \\ \left. - b_{KN}(r) \frac{(\vec{\nabla} \rho(r))^2}{36 \rho(r)} + \vec{\nabla}_{\vec{r}} b_{KN}(r) \rho(r) \cdot \vec{\nabla}_{\vec{r}} \right) \delta^3(\vec{r} - \vec{r}') + \mathcal{O}(\hbar^4) , \quad (16) \end{aligned}$$

where we did not include a spin-orbit force for simplicity (see e.g. [20]). We turn to  $c_{KN}$  in (10). This term appears most susceptible to shell effects since it probes the shell model energies  $E_n$  explicitly. Again we perform the semi-classical expansion

$$\sum_n E_n \chi_n^\dagger(\vec{r}) \chi_n(\vec{r}) = \left( m_N + \bar{\mu} - \frac{\Delta}{18 m_N} - \frac{k_F^2(r)}{5 m_N} \right) \rho(r) + \mathcal{O}(\hbar^4) \quad (17)$$

with  $\bar{\mu} \simeq -8$  MeV the one-nucleon separation energy of the nucleus. This leads to a description of  $K^-$  atoms in terms of the empirical nuclear density profile.<sup>4</sup>

---

<sup>4</sup> We point out that here we exploit the fact that for relevant densities we need only a few terms in the Taylor expanded amplitude in (10). If an infinite sum of terms would be required we could not trust our semi-classical expansion since small shell effects in the coefficients might sum up to large uncertainties.

It is now straightforward to derive the optical potential induced by (10). We obtain:

$$\begin{aligned}
2\mu U_{\text{opt.}}(\omega, \vec{r}, \vec{\nabla}) = & -4\pi \left(1 + \frac{m_K}{m_N}\right) \left(\bar{a}_{KN}[\rho(r)] \rho(r) + s_{KN}[\rho(r)]\right) \\
& + 4\pi \left(1 + \frac{m_K}{m_N}\right) \vec{\nabla} b_{KN}[\rho(r)] \rho(r) \cdot \vec{\nabla} \\
& + 4\pi \left(1 + \frac{m_K}{m_N}\right) (\omega - V_{\text{e.m.}}(r) - m_K) c_{KN}[\rho(r)] \rho(r), \quad (18)
\end{aligned}$$

where we represent the non-local optical potential,  $U_{\text{opt.}}(\vec{r}, \vec{r}')$ , in terms of the differential operator,  $U_{\text{opt.}}(\vec{r}, \vec{\nabla})$ , with:

$$U_{\text{opt.}}(\omega, \vec{r}, \vec{\nabla}) \phi(\vec{r}) = \int d^3 r' U_{\text{opt.}}(\omega, \vec{r}, \vec{r}') \phi(\vec{r}') . \quad (19)$$

We further introduce the renormalized effective scattering length  $\bar{a}_{KN}[\rho]$  and a term  $s_{KN}[\rho]$  responsible for binding and surface effects

$$\begin{aligned}
\bar{a}_{KN}[\rho] &= a_{KN}(\rho) + \frac{3}{5} k_F^2 \left( b_{KN}(\rho) - \frac{1}{2m_N} c_{KN}(\rho) \right), \\
s_{KN}[\rho] &= \frac{1}{12} b_{KN}(\rho) \left( \Delta \rho + \frac{(\vec{\nabla} \rho)^2}{3\rho} \right) - \frac{1}{4} \Delta b_{KN}(\rho) \rho \\
&\quad - c_{KN}(\rho) \left( \bar{\mu} - \frac{k_F^2}{2m_N} - \frac{\Delta}{18m_N} \right) \rho. \quad (20)
\end{aligned}$$

Equation (20) is instructive since it suggests to identify  $\bar{a}_{KN}(\rho)$  with the effective scattering length  $a_{\text{eff.}}(k_F)$  introduced when analyzing the kaon self energy. In fact, we arrive at our final form of the optical potential by replacing  $\bar{a}_{KN}$ ,  $b_{KN}$  and  $c_{KN}$  in (18) by the appropriate functions  $a_{\text{eff.}}(k_F)$ ,  $b_{\text{eff.}}(k_F)$  and  $c_{\text{eff.}}(k_F)$  as extracted from the kaon self energy of the self consistent calculation in [1]. We point out that by replacing

$$\begin{aligned}
\bar{a}_{KN}(\rho) &\rightarrow a_{\text{eff.}}(k_F), & b_{KN}(k_F) &\rightarrow b_{\text{eff.}}(k_F)/k_F, \\
c_{KN}(\rho) &\rightarrow c_{\text{eff.}}(k_F)/k_F, \quad (21)
\end{aligned}$$

in (18) the terms in the optical potential induced by higher order terms in the expanded amplitude (10) are recovered. Here we systematically drop terms involving more than two powers of the differential operator  $\vec{\nabla}$ . Note also that (20) is written in such a way that  $\bar{a}_{KN}$  includes the trivial renormalization of the scattering length implied by (12). This justifies the identification of  $\bar{a}_{KN}$  with  $a_{\text{eff.}}(k_F)$  since it avoids the double inclusion of such effects. The non-trivial

renormalization collected in  $s_{KN}$  then leads to rather sizeable renormalization effects in the effective potential  $V(r)$  (see (23)).

We present the final radial differential equation for the kaon wave function  $\phi(\vec{r}) = \chi(r) Y_{lm}(\theta, \phi)/r$  as it follows from (18,20) and (21):

$$Z(r) \left( \frac{d^2}{dr^2} - \frac{l(l+1)}{r^2} \right) \chi(r) = \bar{Z}(r) \left[ \mu^2 - \left( \mu - E - \frac{i}{2} \Gamma - V_{\text{e.m.}}(r) \right)^2 \right] \chi(r) + 2\mu V(r) \chi(r) + 2\mu S(r) \left( \frac{d}{dr} \chi(r) \right) \quad (22)$$

with

$$\begin{aligned} 2\mu V(r) &= -\frac{8}{3\pi} \left( 1 + \frac{m_K}{m_N} \right) \left[ \frac{1}{4} \left( \frac{2d}{r dr} - \frac{d^2}{dr^2} \right) k_F^2(r) b_{\text{eff.}}(k_F(r)) \right. \\ &\quad + a_{\text{eff.}}(k_F(r)) k_F^3(r) - k_F^2(r) c_{\text{eff.}}(k_F(r)) \left( \bar{\mu} - \frac{k_F^2}{2m_N} \right) \\ &\quad + \left( \frac{k_F(r)}{2r} k'_F(r) + \frac{k_F(r)}{4} k''_F(r) + \frac{3}{4} (k'_F(r))^2 \right) b_{\text{eff.}}(k_F(r)) \\ &\quad \left. + \left( \frac{k_F(r)}{3m_N r} k'_F(r) + \frac{k_F(r)}{6m_N} k''_F(r) + \frac{1}{3m_N} (k'_F(r))^2 \right) c_{\text{eff.}}(k_F(r)) \right], \\ Z(r) &= 1 - \frac{8}{3\pi} \left( 1 + \frac{m_K}{m_N} \right) k_F^2(r) b_{\text{eff.}}(k_F(r)), \\ 2\mu S(r) &= \frac{8}{3\pi} \left( 1 + \frac{m_K}{m_N} \right) \frac{d}{dr} k_F^2(r) b_{\text{eff.}}(k_F(r)), \\ \bar{Z}(r) &= 1 - \frac{8}{3\pi} \left( 1 + \frac{m_K}{m_N} \right) \frac{k_F^2(r)}{2m_K} c_{\text{eff.}}(k_F(r)). \end{aligned} \quad (23)$$

The effective Klein-Gordon equation (22) shows a wave function renormalization  $Z(r)$ , a mass renormalization  $\bar{Z}(r)$  and a surface interaction strength  $S(r)$ . Note that in (22) we approximated the linear energy dependence of (18) by a quadratic one.

We discuss the effect of the semi-classical optical potential (22) at hand of a  $K^-$  bound at the  $^{12}_6\text{C}$ -core and  $^{58}_{28}\text{Ni}$ -core. We use the unfolded density profiles of [11,3]:

$$\begin{aligned} \rho_{[^{12}_6\text{C}]}(r) &= \rho_0 \left( 1 + 2.234 \left( \frac{r}{1.516 \text{ fm}} \right)^2 \right) \exp \left( - \left( \frac{r}{1.516 \text{ fm}} \right)^2 \right), \\ \rho_{[^{58}_{28}\text{Ni}]}(r) &= \rho_0 \left( 1 + \exp \left( \frac{r - 4.134 \text{ fm}}{0.500 \text{ fm}} \right) \right)^{-1}, \end{aligned} \quad (24)$$

with  $\rho_0$  determined by  $4\pi \int dr r^2 \rho(r) = 12$  for carbon and  $4\pi \int dr r^2 \rho(r) = 58$  for nickel. In Fig. 3 the effective potential  $V(r)$ , the effective surface function  $S(r)$  and the renormalization functions  $Z(r), \bar{Z}(r)$  defined in (23) are shown for the  $^{58}_{28}\text{Ni}$  density profile of (24). We point out that for the wave function and mass renormalization functions  $Z(r)$  and  $\bar{Z}(r)$  we find quite large deviations of about 50% from the asymptotic value 1. Also the function  $S(r)$  shows sizeable strength close to the nucleus surface. Note also that the effective potential  $V(r)$  receives a large contribution proportional to  $c_{\text{eff.}}(k_F)$  which almost doubles the value of  $\Re V(0)$  as compared to  $\Re V(0)$  as it would follow with  $c_{\text{eff.}} = 0$ . Obviously such effects must not be ignored.

We introduce the nuclear level shift,  $\Delta E_{\text{nucl.}}$ , in terms of the measured transition energy,  $\Delta E_{\text{emp.}} = \Delta E_{\text{e.m.}} + \Delta E_{\text{nucl.}}$ , and the theoretical electromagnetic transition energy,  $\Delta E_{\text{e.m.}}$ . For the  $^{12}_6\text{C} K^-$  system we consider the  $3\text{d} \rightarrow 2\text{p}$  transition with  $E_{\text{e.m.}}(2\text{p}) = 0.113763$  MeV and  $E_{\text{e.m.}}(3\text{d}) = 0.050458$  MeV. For the  $^{58}_{28}\text{Ni} K^-$  system we consider the  $5\text{g} \rightarrow 4\text{f}$  transition with  $E_{\text{e.m.}}(4\text{f}) = 0.641572$  MeV and  $E_{\text{e.m.}}(5\text{g}) = 0.409951$  MeV. Here the Coulomb potential and the vacuum polarization potentials [10] are folded with the nucleus density profile (24). We use here  $m_{K^-} = 493.677$  MeV and  $1/\alpha = 137.035989$ . The empirical transition energy is  $\Delta E_{\text{emp.}} = 62.73 \pm 0.08$  keV with  $\Gamma = 1.73 \pm 0.15$  keV [13] for carbon and  $\Delta E_{\text{emp.}} = 231.408 \pm 0.052$  keV with  $\Gamma = 1.230 \pm 0.140$  keV for nickel. Note that the resulting empirical nuclear level shifts  $\Delta E_{\text{nucl.}} =$

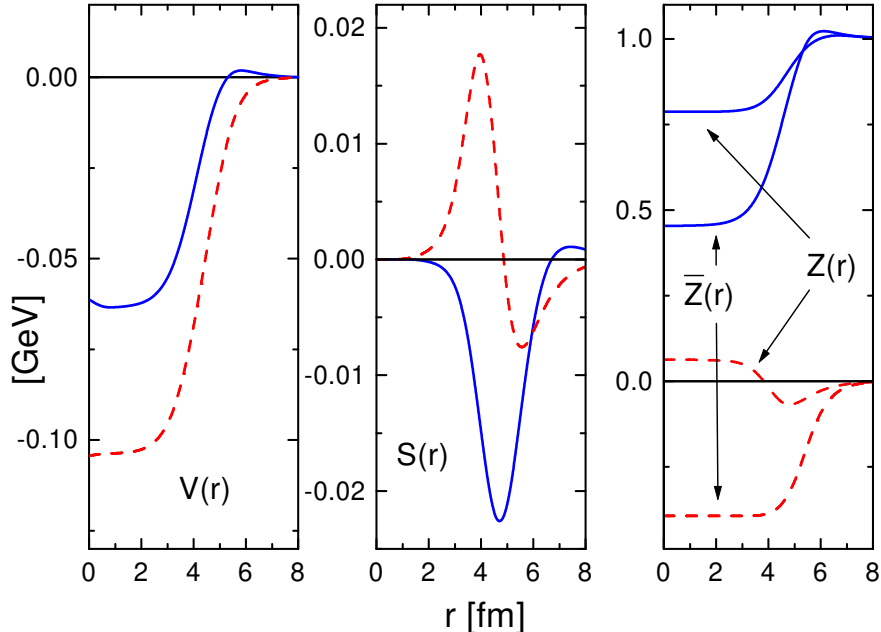


Fig. 3. The effective potential  $V(r)$ , the effective surface function  $S(r)$  and the effective renormalization functions  $Z(r), \bar{Z}(r)$  as introduced in (23) for the  $^{58}_{28}\text{Ni} K^-$  system. The solid and dashed lines represent the real and imaginary parts respectively.

	$^{12}_6\text{C}$ (3d→2p)		$^{58}_{28}\text{Ni}$ (5g→4f)	
	$-\Delta E_{\text{nucl.}}$ [eV]	$\Gamma$ [eV]	$-\Delta E_{\text{nucl.}}$ [eV]	$\Gamma$ [eV]
$a_{KN} = (-0.18 + i 0.67)$ fm	475	761	199	476
$a_{KN}^{(\text{eff.})} = (0.63 + i 0.89)$ fm	593	1362	143	932
$b_{\text{eff.}} = 0$ & $c_{\text{eff.}} = 0$	603	1022	248	627
$c_{\text{eff.}} = 0$	701	1083	347	759
full theory	854	1125	437	847
experiment [13,21]	$590 \pm 80$	$1730 \pm 150$	$246 \pm 52$	$1230 \pm 140$

Table 2

Results for the  $^{12}_6\text{C}$  K $^-$  and  $^{58}_{28}\text{Ni}$  K $^-$  systems. The first two rows show the results from the optical potential (1) with i) the empirical repulsive scattering length  $a_{KN} = (-0.18 + i 0.67)$  fm and ii) the effective attractive scattering length  $a_{KN}^{(\text{eff.})} = (0.63 + i 0.89)$  fm. The remaining rows show the result with the semi-classical optical potential (23) with iii)  $b_{\text{eff.}} = 0 = c_{\text{eff.}}$ , iv) with  $c_{\text{eff.}} = 0$  and v) with  $a_{\text{eff.}}$ ,  $b_{\text{eff.}}$  and  $c_{\text{eff.}}$  from Fig. 2.

$-573 \pm 80$  keV for carbon and  $\Delta E_{\text{nucl.}} = -213 \pm 52$  keV for nickel differ slightly from the values given in [13,21] and shown in Tab. 2. The reason for which is an old value for the kaon mass, a slightly different nucleus profile and the inclusion of further small correction terms.

In Tab. 2 we compare the results from the low-density optical potential (1) with the result of the semi-classical optical potential. Neither the full semi-classical potential nor a reduced form where we neglect the wave function renormalization is able to reproduce the empirical level shifts satisfactorily. As can be seen from Tab. 2 again the non-local effects are sizeable and must not be ignored. The results obtained with the semi-classical potential differ significantly from any of the phenomenological potentials (7) with an ad-hoc gradient ordering. We emphasize that the crucial assumption of our approach, namely that the results are insensitive to the precise form of the slope functions  $b_{\text{eff.}}(k_F)$  and  $c_{\text{eff.}}(k_F)$  in the extreme surface region  $k_F < q \simeq 20$  MeV, which justifies the expansion (4), is fulfilled. The size of the level shifts, using  $b_{\text{eff.}}(k_F)$  and  $c_{\text{eff.}}(k_F)$  functions modified according to (8), are reduced by about 5% in  $^{12}_6\text{C}$  K $^-$  and by about by 10% in  $^{58}_{28}\text{Ni}$  K $^-$ . The level widths are affected by at most 5 %. Note that this uncertainty is not resolved by the accuracy of the available empirical level shifts.

## 5 Summary

We summarize the findings of our work. The kaon self energy shows a rapid density, energy and momentum dependence in nuclear matter. This rich structure is a consequence of a proper many-body treatment of the  $\Lambda(1405)$  resonance structure in nuclear matter invalidating any mean field type approach to kaon propagation in nuclear matter at moderate densities. Thus non-local terms in the optical potential are large and quantitatively important. If included in the calculation of the kaonic atom spectra they cause substantial additional shifts of the binding energies and level widths. Since the kaon self energy must be obtained in a non-perturbative many-body approach it is not immediate as to which gradient ordering to choose. A phenomenological p-wave like ordering of gradient terms with the strength taken from the many-body calculation of [1,15] leads to a satisfactory description of the kaonic atom level shifts. We point out, however, that a proper microscopic description of  $K^-$ -atom data requires a careful derivation of the non-local part of the optical potential. We suggest to determine the gradient ordering systematically by applying a semi-classical expansion to the nucleus structure. At present this approach fails to reproduce the empirical level shifts. We emphasize that the kaonic atom data appear very sensitive to the precise microscopic interaction of the kaon-nucleon system. From the fact that the semi-classical optical potential derived from the s-wave dynamics of [1] does not yet lead to a satisfactory description of the level shifts we conclude that an improved microscopic input for the many-body calculation of the kaon self energy is required. This is supported by the recent chiral  $SU(3)$  analysis of the kaon-nucleon scattering data which includes for the first time also p-wave effects systematically [18]. It is found that the subthreshold kaon-nucleon scattering amplitudes differ strongly from those of [8,15] and that p-wave effects in the isospin one channel are strong. An evaluation of the many-body effects based on the improved chiral  $SU(3)$ -dynamics is in progress [22].

## Acknowledgments

W.F. thanks the members of the Theory Group at GSI for very warm hospitality. M.L. acknowledges partial support by the Polish Government Project (KBN) grant 2P03B00814.

## 6 Appendix

In this appendix we derive the contribution from Pauli blocking to the in-medium kaon-nucleon scattering process and the kaon self energy. Pauli blocking induces a model independent term in the scattering amplitude  $T_{KN}^{(P.B.)}(\omega + m_N, \vec{q})$  and self energy  $\Pi_K^{(P.B.)}(\omega, \vec{q})$  proportional to the squared s-wave scattering lengths:

$$T_{KN}^{(P.B.)}(\omega + m_N, \vec{q}) = \pi (1 + \kappa) \left( \left( a_{KN}^{(0)} \right)^2 + 3 \left( a_{KN}^{(1)} \right)^2 \right) I(\omega, \vec{q}) ,$$

$$\Pi_K^{(P.B.)}(\omega, \vec{q}) = -4 \int_0^{k_F} \frac{d^3 p}{(2\pi)^3} T_{KN}^{(P.B.)}(\omega + m_N + p^2/(2m_N), \vec{p} + \vec{q}) , \quad (25)$$

with  $\kappa = m_K/m_N$  and

$$I(\omega, \vec{q}) = i p_{\text{cm}}[\omega, \vec{q}]$$

$$- \int_0^{k_F} \frac{d^3 l}{(2\pi)^3} \frac{4\pi(1+\kappa)}{m_K^2 + \Delta m_K^2 - \omega^2 + (1 + \omega/m_N) \vec{l}^2 - 2 \vec{l} \cdot \vec{q} + \vec{q}^2 - i\epsilon} ,$$

$$\sqrt{(\omega + m_N)^2 - \vec{q}^2} = \sqrt{m_N^2 + p_{\text{cm}}^2[\omega, \vec{q}]} + \sqrt{m_K^2 + \Delta m_K^2 + p_{\text{cm}}^2[\omega, \vec{q}]} . \quad (26)$$

Note that in the denominator of (26) we neglected relativistic correction terms of the form  $(l^2)^{n+1}/m_N^{2n}$  or  $\omega (l^2)^{n+1}/m_N^{2n+1}$  with  $n \geq 1$  but kept the correction term  $\omega/m_N$ . The latter term is important since it renders the derivatives  $\partial_\omega \Pi(m_K, 0)$  and  $\partial_{q^2} \Pi(m_K, 0)$  finite and well defined at  $\omega = m_K$  and  $q^2 = 0$ . We emphasize that the inclusion of the kaon mass modification  $\Delta m_K^2 \sim k_F^3$  as required in a self-consistent calculation [1] leads to a well defined behavior of  $I(\omega, \vec{q})$  close to  $\omega \simeq m_K$  and  $\vec{q} \simeq 0$ . Similarly, as suggested in [23], one may include nuclear binding effects in  $I(\omega, \vec{q})$  by replacing  $m_N \rightarrow m_N + \Delta m_N$  and  $\omega \rightarrow \omega - \Delta m_N$  in the r.h.s of (26). This leads to identical results for the low-density limits  $\partial_\omega T(m_K + m_N, 0)$  and  $\partial_{q^2} T(m_K + m_N, 0)$  since only the combination  $\Delta m_K + \Delta m_N$  is active at leading order and will cancel identically. It is straightforward to derive:

$$\frac{\partial}{\partial \omega} I(m_K, 0) = \frac{4}{\pi} \frac{m_K}{k_F} \frac{1}{1 + \kappa} + \mathcal{O}(k_F^0) ,$$

$$\frac{\partial}{\partial q^2} I(m_K, 0) = -\frac{2}{3\pi} \frac{1}{k_F} \frac{3\kappa - 1}{(1 + \kappa)^2} + \mathcal{O}(k_F^0) , \quad (27)$$

leading to our result (11). Note that the two terms in  $I(\omega, \vec{q})$  lead to contributions proportional to  $1/\sqrt{\Delta m_K + \Delta m_N}$  in (27) which however cancel identically. Similarly one may expand

$$\begin{aligned}
\int_0^{k_F} \frac{d^3 p}{(2\pi)^3} I(m_K + p^2/(2m_N), \vec{p}) &= -\frac{k_F^4}{4\pi^3} \frac{1 - \kappa^2 + \kappa^2 \ln \kappa^2}{(1 - \kappa)^2 (1 + \kappa)} + \mathcal{O}(k_F^5) , \\
\frac{d}{d\omega} \bigg|_{\omega=m_K} \int_0^{k_F} \frac{d^3 p}{(2\pi)^3} I(\omega + p^2/(2m_N), \vec{p}) &= -\frac{k_F^2 m_K}{2\pi^3} \frac{\ln |\kappa|}{1 + \kappa} + \mathcal{O}(k_F^3) , \\
\frac{d}{dq^2} \bigg|_{q^2=0} \int_0^{k_F} \frac{d^3 p}{(2\pi)^3} I(m_K + p^2/(2m_N), \vec{p} + \vec{q}) &= \frac{k_F^2}{4\pi^3} \left( \frac{7}{3} \frac{\ln |\kappa|}{1 + \kappa} \right. \\
&\quad \left. + \frac{2}{3} \frac{1 - \kappa^2 + 2\kappa^2 \ln |\kappa|}{(1 + \kappa)(1 - \kappa)^2} \right) + \mathcal{O}(k_F^3) , \tag{28}
\end{aligned}$$

and arrive at the low-density limit of  $b_{\text{eff.}}(0)$  and  $c_{\text{eff.}}(0)$  as given in (5). For completeness we included in (28) the integral leading to the  $k_F^4$ -term in the self energy given in [1]. Its limit for small  $\kappa$  was derived in [24].

## References

- [1] M. Lutz, Phys. Lett. **B 426** (1998) 12; M.F.M. Lutz, in *Proc. Workshop on Astro-Hadron Physics*, Seoul, Korea, October, 1997, nucl-th/980233.
- [2] E. Friedmann, A. Gal and C.J. Batty, Phys. Rep. **287** (1997) 385.
- [3] E. Friedman, A. Gal and C.J. Batty, Nucl. Phys. **A 579** (1994) 518.
- [4] M. Thies, Nucl. Phys. **A 298** (1978) 344.
- [5] M. Mizoguchi, S. Hirenzaki and H. Toki, Nucl. Phys. **A 567** (1994) 893; Nucl. Phys. **A 585** (1995) 349c.
- [6] R. Brockmann and W. Weise, Nucl. Phys. **A 308** (1978) 365.
- [7] E. Friedman, A. Gal, J. Mares and A. Cieply, Phys. Rev. **C 60** (1999) 024314.
- [8] T. Waas, N. Kaiser and W. Weise, Phys. Lett. **B 365** (1996) 12.
- [9] V. Koch, Phys. Lett. **B 337** (1994) 7; A. Ohnishi, Y. Nara and V. Koch, Phys. Rev. **C 56** (1997) 2767.
- [10] J. Blomqvist, Nucl. Phys. **B 48** (1972) 95.
- [11] H. de Vries, C.W. de Jaeger and C. Vries, Atomic Data and Nuclear Data **36** (1987) 495.
- [12] M. Krell and T.E.O. Ericson, Jour. Comp. Phys. **3** (1968) 202.
- [13] G. Backenstoss, A. Bamberger, I. Bergström, P. Bounin, T. Bunaciu, J. Egger, S. Hultberg, H. Koch, M. Krell, U. Lynen, H.G. Ritter, A. Schwitter, and R. Stearns, Phys. Lett. **B 38** (1972) 181.

- [14] P.D. Barnes, R.A. Eisenstein, W.C. Lam, J. Miller, R.B. Sutton, M. Eckhouse, J.R. Kane, R.E. Welsh, D.A. Jenkins, R.J. Powers, A.R. Kuselman, R.P. Redwine and R.E. Segel, Nucl. Phys. **A** **231** (1974) 477.
- [15] A. Ramos and E. Oset, Nucl. Phys. **A** in print; nucl-th/9906016; we thank A. Ramos for providing us with a table of their effective scattering length.
- [16] A. Baca, C. Garcia-Recio and J. Nieves, nucl-th/0001060.
- [17] S. Hirenzaki, Y. Okumura, H. Toki, E. Oset and A. Ramos, Phys. Rev. **C** in print; we thank A. Ramos for communicating the above manuscript prior to publication.
- [18] M.F.M. Lutz and E.E. Kolomeitsev, in *Proceedings of the International Workshop XXVII on Gross Properties of Nuclei and Nuclear Excitations*, Hirschegg, Austria, January, 2000.
- [19] L.S. Kisslinger Phys. Rev. **98** (1955) 761.
- [20] M. Brack, C. Guet and H.-B. Hakansson, Phys. Rep. **123** (1985) 276.
- [21] C. J. Batty, S.F. Biagi, M. Blecher, S.D. Hoath, R.A.J. Riddle, B.L. Roberts, J.D. Davies, G.J. Pyle, G.T.A. Squier, D.M. Asbury, A.S. Clough, Nucl. Phys. **A** **329** (1979) 407.
- [22] C. Korpa and M. Lutz, in preparation.
- [23] C. Garcia-Reio, L.L. Salcedo and E. Oset, Phys. Rev. **C** **39** (1989) 595.
- [24] C. Garcia-Recio, E. Oset, L.L. Salcedo, Phys. Rev. **C** **37** (1988) 194.